AD A044450

Small-Scale CW HF(DF) Chemical Laser

Aerophysics Laboratory
The Ivan A. Getting Laboratories
The Aerospace Corporation
El Segundo, Calif. 90245

3 August 1977

Interim Report
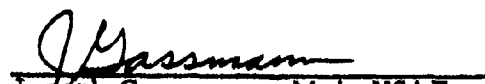
D D C

SEP 22 1977

B

This interim report was submitted by The Aerospace Corporation, El Segundo, CA 90245, under Contract No. F04701-76-C-0077 with the Space and Missile Systems Organization, Deputy for Advanced Space Programs, P.O. Box 92960, Worldway Postal Center, Los Angeles, CA 90009. It was reviewed and approved for The Aerospace Corporation by W. R. Warren, Jr., Director, Aerophysics Laboratory. Lieutenant A. G. Fernandez, SAMSO/YAPT, was the project officer for Advanced Space Programs.

This report has been reviewed by the Information Office (OI) and is releasable to the National Technical Information Service (NTIS). At NTIS, it will be available to the general public, including foreign nations.

This technical report has been reviewed and is approved for publication. Publication of this report does not constitute Air Force approval of the report's findings or conclusions. It is published only for the exchange and stimulation of ideas.

Arturo G. Fernandez, 1st Lt, USAF
Project Officer

Joseph Gassmann, Maj, USAF

FOR THE COMMANDER

LEONARD E. BALTZELL, Col, USAF, Asst.
Deputy for Advanced Space
Programs

REPORT DOCUMENTATION PAGE		READ INSTRUCTIONS BEFORE COMPLETING FORM
1. REPORT NUMBER SAMSO-TR-77-153	2. GOVT ACCESSION NO.	3. RECIPIENT'S CATALOG NUMBER
4. TITLE (and Subtitle) SMALL-SCALE CW HF(DF) CHEMICAL LASER.		5. TYPE OF REPORT & PERIOD COVERED Interim
		6. PERFORMING ORG. REPORT NUMBER TR-0077(2940)-4
7. AUTHOR(s) Donald J. Spencer, James A. Beggs and Harold Mirels		8. CONTRACT OR GRANT NUMBER(s) F04701-76-C-0077
9. PERFORMING ORGANIZATION NAME AND ADDRESS The Aerospace Corporation El Segundo, Calif. 90245		10. PROGRAM ELEMENT, PROJECT, TASK AREA & WORK UNIT NUMBERS
11. CONTROLLING OFFICE NAME AND ADDRESS Space and Missile Systems Organization Air Force Systems Command Los Angeles, Calif. 90009		12. REPORT DATE 3 August 1977
		13. NUMBER OF PAGES 37
14. MONITORING AGENCY NAME & ADDRESS(if different from Controlling Office)		15. SECURITY CLASS. (of this report) Unclassified
		15a. DECLASSIFICATION/DOWNGRADING SCHEDULE

16. DISTRIBUTION STATEMENT (of this Report)

Approved for public release; distribution unlimited

DDC
RECEIVED
SEP 22 1977
B

17. DISTRIBUTION STATEMENT (of the abstract entered in Block 20, if different from Report)

18. SUPPLEMENTARY NOTES

19. KEY WORDS (Continue on reverse side if necessary and identify by block number)

HF Laser　　　　　　　　CW Chemical Laser
DF Laser　　　　　　　　HF (DF) Probe Laser
Chemical Laser

20. ABSTRACT (Continue on reverse side if necessary and identify by block number)

The construction and performance of a small-scale cw HF(DF) chemical laser is described. A multiline output of about 15 W (8 W) was achieved. During single-line operation, 18 HF 2-1 and 1-0 transition lines, with powers from 0.1 to 2.4 W, and 24 DF 3-2, 2-1 and 1-0 transition lines, with powers from 0.01 to 0.30 W, were observed. Amplitude stability varied from ±1.5% to ±5%, and free-running short-term frequency stability was about ±10 MHz.

DD FORM 1473
(FACSIMILE)

409367

PREFACE

The many helpful discussions with Dr. J. Hinchen during the initial design of the laser are gratefully appreciated.

CONTENTS

FIGURES

TABLES

I. INTRODUCTION

Continuous-wave HF and DF chemical lasers have the potential for high output power; devices with output powers of the order of 1 kW have been reported.[1] However, there is a need for a small-scale (i.e., output power on the order of 1 W) amplitude- and frequency-stable cw chemical laser for a variety of applications. These applications include such chemical laser diagnostic studies as small-signal-gain measurements,[2] atmospheric propagation, and window-material and optic-coating development. A stable HF(DF) laser is also needed for use as the local oscillator in a laser-sun heterodyne radiometer detection array employed in high-resolution atmospheric-transmission measurements.[3]

The use of small-scale chemical lasers for diagnostic studies was reported by Cool[4] and Hinchen.[5] Cool used a microwave discharge to generate F atoms, whereas Hinchen used a dc discharge. The construction and performance of a small-scale cw HF(DF) laser that is similar to the device described by Hinchen is described here.

II. LASER DESIGN

The laser is shown in Figs. 1 and 2. The device can be divided conveniently into the five regions (i.e., the discharge region, inlet region, lasing zone, heat exchanger, and exhaust). The discharge region provides an F-atom flow for the chemical reaction by means of a high-voltage discharge in a water-cooled pyrex tube containing SF_6, He, and O_2 that generates vibrationally excited HF or DF molecules. The He serves as a thermal diluent (and also reduces the required discharge voltage), whereas the SF_6 is the F-atom source. Oxygen is added to the flow to increase the F-atom concentration and to eliminate S deposition through exothermic reaction with the S atoms formed in the discharge. The mixed gases are injected into one end of the discharge tube upstream of a group of eight symmetrically deployed 1/16-in.-diameter by 6-in.-long Ni wires that serve as discharge anodes. The operation of the Ni wires as cathodes resulted in metal loss and reduced power output. The discharge uniformity depends heavily upon the flow uniformity of the gases at the electrode tips; therefore, the gas injection into the discharge tube is made as uniform as possible. The long anodes are gas-cooled in the region upstream of the discharge. The Ni anodes are individually connected through ballast resistors (50 kΩ, 100 kΩ, or 200 kΩ) to the positive terminal of the power supply. The ballast resistor values can be varied to accommodate power-supply characteristics and laser operating conditions. The ballast resistor bank is forced-air-cooled.
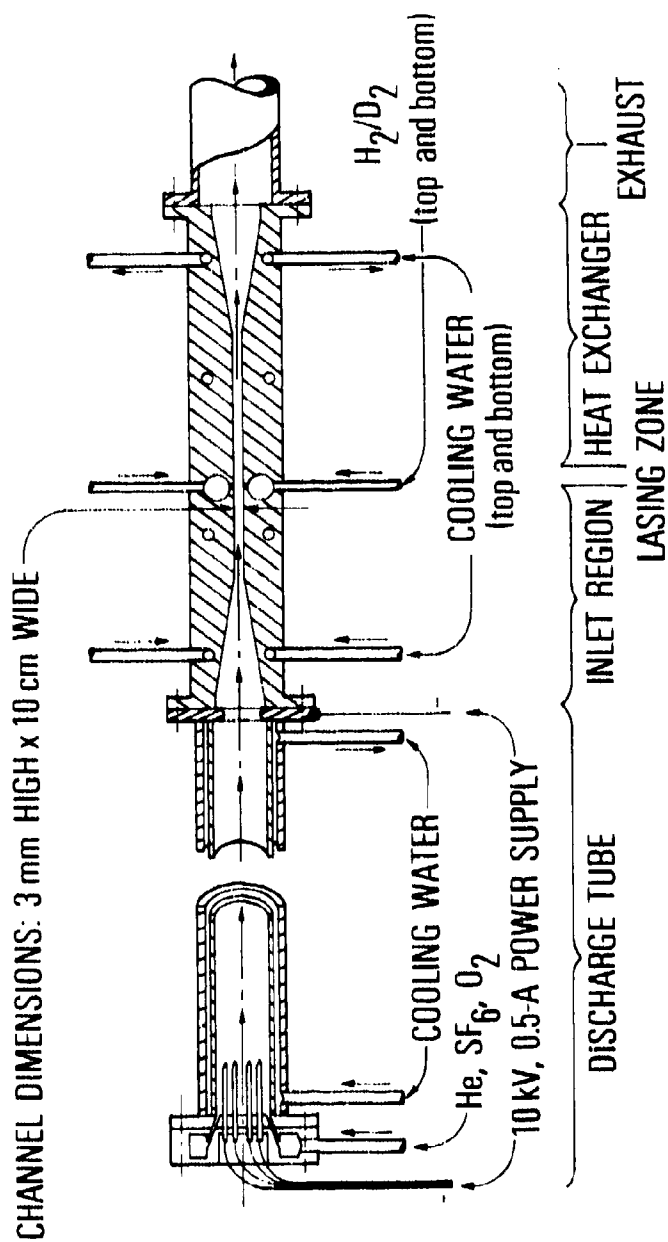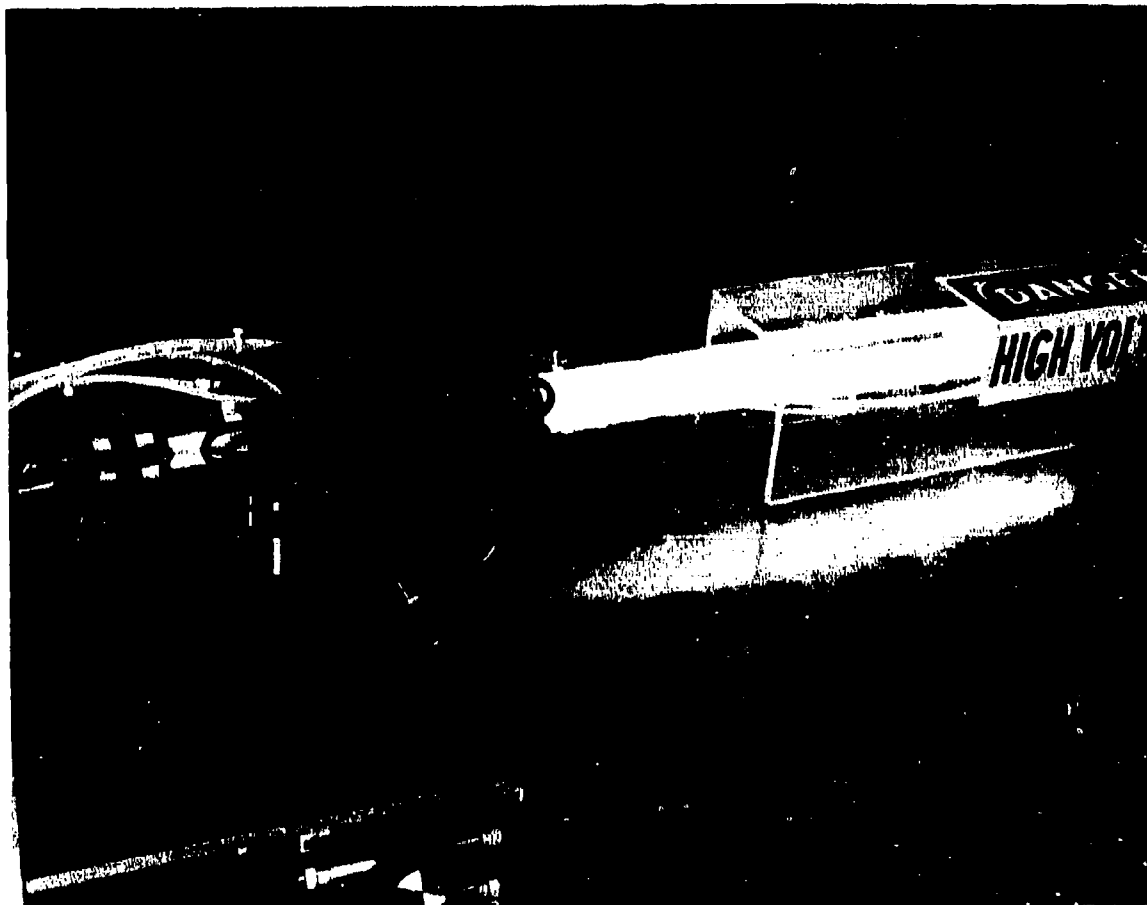
Figure 1. Stable HF(DF) Chemical Laser

Figure 2.   Laser Discharge Tube and Cavity

The discharge takes place along a central core in the pyrex tube and terminates on a water-cooled Cu hole electrode (3/4-in. diameter) at the entrance to the laser inlet region. The pyrex tube has a 1-in. i.d., 0.062-in. wall thickness and nominally is used in two lengths, 12 and 24 in., with 10- and 20-kV power supplies, respectively. An Al_2O_3 cylindrical shell is inserted inside the pyrex tube at the junction with the cathode to eliminate discharge attachment at the pyrex-Cu cathode interface. The water jacket surrounding the pyrex tube is made of lucite.

The hot flow containing F atoms passes through the cathode hole into the inlet region where the flow cross section is changed from a square geometry of the same nominal cross section as the discharge tube to the channel cross section 10 by 0.3 cm. The H_2 is injected along a line transverse to the flow at both the top and bottom of the channel through 40 evenly spaced 0.0135-in.-diameter holes in each wall. The H_2 is fed from plenums immediately above and below the injection hole array. The lasing zone is immediately downstream of the H_2 injection ports, where the mixing of the H_2 and F takes place. The remaining portion of the channel downstream of this region and the transition section in which the rectangular channel geometry is returned to a circular geometry for convenience in ducting serve as a heat exchanger to reduce the temperature of the heated gas to ~200°C. Further temperature reduction of the gas is accomplished in a downstream heat exchanger.

The inlet region, the mixing and lasing zone, and the heat exchanger are fabricated in a single Amsulf Cu block 8 by 4 by 1-1/2 in. The assembly is water-cooled and contains the H_2 plenums. The laser is exhausted to a 150

cfm) vacuum pump through a conventional 1-1/2 in. i.d. flexible vacuum hose. A surge tank in the exhaust is unnecessary for damping pump pressure fluctuations since no pressure variations at the laser are detectable with the undamped system operating at normal flow rates. Brewster-angle BaF_2 windows are mounted on channel sidewalls that are O-ring sealed to the channel body. The windows are centered along the gain region in the channel, nominally, 1-mm downstream of the H_2 injection holes. Laser-beam polarization can be controlled by the rotation of the Brewster-angle windows for proper orientation with respect to the gratings. In an early experiment, a small purge flow of He was injected at the Brewster windows to reduce the accumulation of ground-state HF or DF, but the use of the flow did not affect laser performance and, hence, was discontinued. The optical cavity is constructed from Burleigh optical erector set components and consists of stainless-steel star gimbal mounts on stainless-steel rod plates that are clamped to four 1-in.-diameter Invar rods. The laser Cu body is suspended between the optical cavity rods with the gain region colinear with the optical-cavity centerline. Multiline power can be coupled from the laser by means of a partially transmitting mirror used in conjunction with a totally reflecting mirror, one of which is a spherical mirror of radius 1 to 10 m and the other, an optical flat. Single-line operation can be accomplished by use of a 300- or 600-lines/mm grating in the autocollimation position with zero-order coupling for lasing at the desired wavelength and with a spherical totally reflecting mirror used as the other cavity component.

III. OPERATING CHARACTERISTICS

The laser is generally used with a 150-cfm vacuum pump and a 20-kV 500-mA power supply. A 24-in. long discharge tube is employed with power supplies of 10 kV or greater terminal voltage. A 12-in.-long discharge tube is used with 5 and 10 kV open-circuit-voltage power supplies capable of operating at ~1 A current levels. Maximum power is obtained with the higher voltage operation, however. Two 100-kΩ, 250-W ballast resistors are connected in series with each of the eight Ni wire electrodes. Thus, the total ballast resistance in series with the discharge is 25 kΩ. This ballast resistance value yields optimum electrical efficiency when used with a 20-kV open-circuit-voltage power supply (50 kΩ/leg is optimum with a 10-kV supply). The multiline HF laser performance for several total-ballast resistance values ranging from 12.5 to 37.5 kΩ and including the electrical-power distribution in the ballast-discharge circuit, the electrical to laser-power conversion efficiency, and the channel operating pressures 1/2-in. upstream of the laser cavity and at the channel exit is given in Table I. Maximum laser power for the standard HF operating condition (Table II) is 12 W. The maximum overall electrical-to-laser power conversion efficiency is obtained with the 25-kΩ ballast resistor and is equal to 1/2%. The power distribution between ballast and discharge is 65/44 for this ballast resistor. The power supply operates at 15.6 kV and 350 mA. Gas pressure is ~23.5 Torr in the laser-cavity region. Gas temperatures can also be measured by means of thermocouples placed in the flow at the channel entrance and exit

Table I. Laser, Ballast Resistor, and Power Supply Operating Characteristics

Ballast Resistance (Ω)	Current (mA)	Load			Power					Pressure	
		Power Supply Terminals (kV)	Ballast Resistor (kV)	Laser Discharge (kV)	Power Supply (kW)	Ballast Resistor (kW)	Laser Discharge (kW)	Laser Output (W)	Efficiency (%)	Total Upstream of Cavity (Torr)	P2 Exit (Torr)
HF LASER[a]											
12.5	500	12.5	6.25	6.25	6.25	3.125	3.125	12.0	0.38	25.5	12.1
18.75	450	14.5	7.5	—	5.89	3.0	2.60	12.3	0.43	25.0	12.0
25.0	350	15.6	8.15	7.45	5.46	3.06	2.40	12.0	0.50	23.4	15.7
37.5	300	12.0	11.25	7.75	5.76	3.375	2.325	10.0[b]	0.43[b]	23.0	16.1
DF LASER[c]											
12.5	500	12.7	6.30	6.40	6.35	3.15	3.20	7.0	0.32	25.0	14.1
18.75	400	14.5	7.50	7.20	5.86	3.00	2.60	7.0	0.24	24.5	14.1
25.0	350	16.4	8.75	7.46	5.74	3.06	2.68	7.0	0.26	24.9	14.0
37.5	260	10.4	9.75	3.65	5.04	2.93	2.51	5.0[c]	0.20[c]	22.0	14.7

[a] Laser operating conditions: 24-in.-long discharge tube; laser cavity : 40-in. radius-of-curvature of total reflector and 15% coupling mirror; $\dot{m}_{He}$ = 0.654; $\dot{m}_{H_2}$ = 0.030; $\dot{m}_{O_2}$ = 0.160; $\dot{m}_{SF_6}$ = 0.170 × sec; power supply : 20 kV open circuit voltage.

[b] Laser output power not optimized because of power supply voltage limitation (20 kV).

[c] Laser operating conditions: 24-in.-long discharge tube; laser cavity : 40-in. radius-of-curvature of total reflector and 7% coupling mirror; $\dot{m}_{He}$ = 0.860; $\dot{m}_{D_2}$ = 0.044; $\dot{m}_{O_2}$ = 0.150; $\dot{m}_{SF_6}$ = 0.190 × sec; power supply : 20 kV open circuit voltage.

Table II. Standard HF Laser Operating Conditions

Electrical Power	Voltage = 15.6 kV, current = 350 mA, R_B = 25 kΩ, 24-in.-discharge tube length
Optical Cavity	40-in.-radius-of-curvature of total reflector and 15% dielectric output coupler separated by 16 in.
Cavity Gas Conditions	Pressure: 1/2 in. upstream of lasing region = 23.5 Torr, channel exit = 15.7 Torr. Temperature: channel entrance = $\sim$1000° K, lasing region = $\sim$700° K, channel exit = $\sim$500° K.
Gas Mass Flow	$\dot{m}_{O_2}$ = 0.180 g/sec $\dot{m}_{He}$ = 0.054 g/sec $\dot{m}_{H_2}$ = 0.026 g/sec $\dot{m}_{SF_6}$ = 0.870 g/sec

and spectrographically in the lasing zone from HF laser line width measurements obtained by the piezoelectric controlled variation of the cavity length. Channel-entrance temperatures are typically $\sim 1000^\circ$K, whereas the lasing zone temperature is $\sim 700^\circ$K. This relatively high laser reaction temperature results in a peaking of the laser lines at rotational quantum number $j = 7$ in HF operation and $j = 10$ in DF operation.

Similar data for DF laser operation are given in Tables I and III. Maximum laser power for the standard DF operating conditions is 7 W. Again, the maximum overall electrical-to-laser power conversion efficiency is obtained with the 25-kΩ ballast resistor and is equal to 0.26%. Power-supply voltage is 16.4 kV, and discharge current is again 350 mA. Gas pressure is ~ 24 Torr and gas temperature $\sim 700^\circ$K.

Maximum multiline laser output power ever observed in this laser is 15 W with SF_6 used as the F-atom source. Substitution of NF_3 for SF_6 results in a 18-W HF and DF laser output. Several attempts were made to increase laser power by redesign, which included increasing the number of the injection holes from 40 to 120 per side, but no net gain in laser power was observed. The laser performance appears to be F-atom-limited and not diffusion-limited. The reduction of performance with mirror, window, or flow degradation is always much greater with the DF laser than the HF because of the lower gain per line in the DF laser.

The static-pressure measurements obtained at entrance and exit points on the channel as well as at the pump entrance flange are given in Fig. 3. Pressure measurements are made 2.5 and 3.0 in. downstream of the

-16-

Table III. Standard DF Laser Operating Conditions

|	
Electrical Power:	Voltage = 16.4 kV, current = 350 mA, R_B = 25 kΩ, 24-in.-discharge tube length
Optical Cavity:	40-in.-radius-of-curvature of total reflector and 7% dielectric output coupler separated by 16 in.
Cavity Gas Conditions	Pressure: 1/2 in. upstream of lasing region = 24.0 Torr, channel exit = 14.0 Torr. Temperature: channel entrance = ~1000°K, lasing region = ~700°K, channel exit = ~500°K.
Gas Mass Flows	$\dot{m}_{O_2}$ = 0.150 g/sec $\dot{m}_{He}$ = 0.0405 g/sec $\dot{m}_{D_2}$ = 0.044 g/sec $\dot{m}_{SF_6}$ = 0.980 g/sec
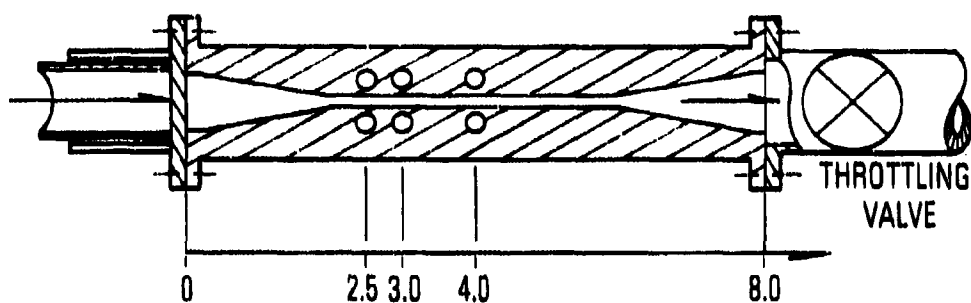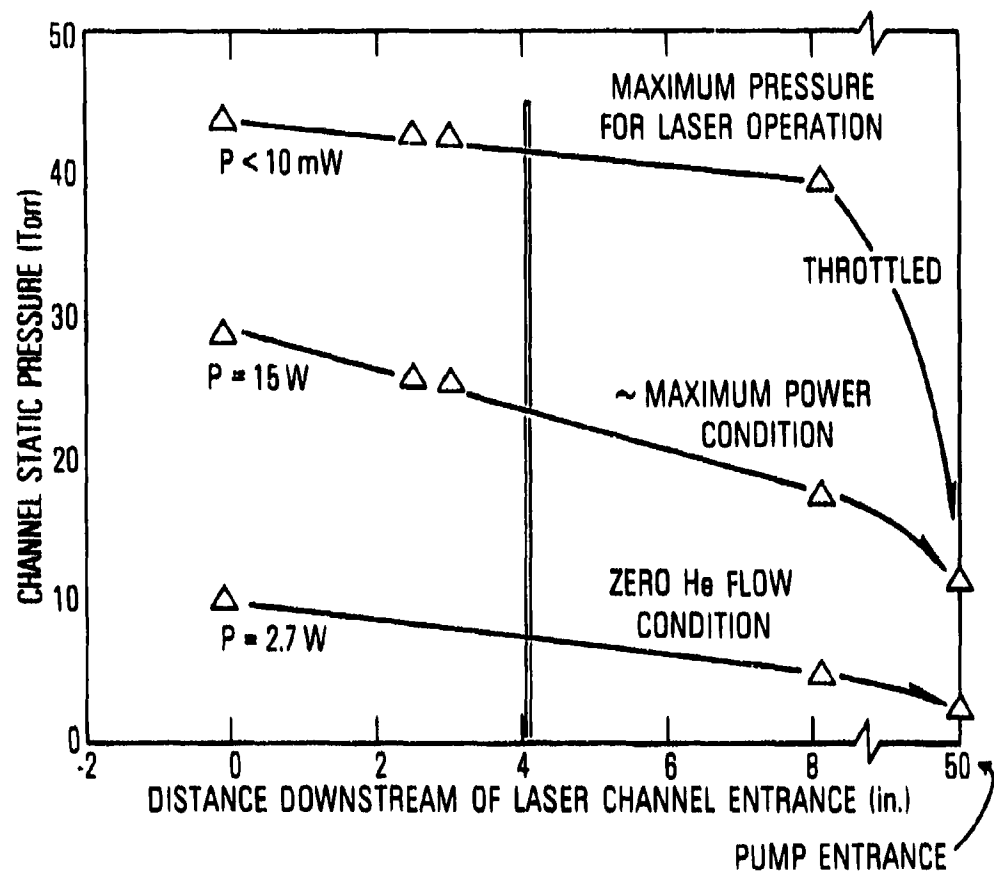
Figure 3. Static Pressure in Channel for Various
Operating Conditions

channel entrance in a channel configuration (cross section, Fig. 3). This con-
figuration is identical to the standard configuration (Fig. 1) except for the
placement of three sets of H_2-injection plenums and the associated 40 injec-
tion holes at each plenum. It is used to determine the dependence of the
laser-power output on the longitudinal injection position of the H_2 in the chan-
nel. However, no significant power difference is observed in this configura-
tion at any of the three locations. Also included in Fig. 3 are the static-
pressure measurements for a zero He flow run condition. Multiline HF power
is measured at 2.7 W for this situation. In addition, the maximum allowed
pressure for laser operation is determined by the downstream throttling of
the flow under maximum power flow conditions. Laser cavity pressure is
~41 Torr at a power level of <10 mW for this condition.

Normalized output power curves for the various gases used in HF-
laser operation are shown in Figs. 4 through 7. The intercepts of the curves
with the ordinate axes indicate the criticality of the various gases in the
lasing process. For example, both O_2 and He curves exhibit lasing at 16%
full power at zero He or O_2 flow, indicating the roles of these gases as
auxiliaries to the fuel and oxidizer. However, the sixfold increase in laser
power resulting from the addition of each of these gases to the flow illus-
trates the importance of the influence of these two gases on F-atom generation
or thermal control, or both. The H_2 intercept is at zero, as expected for
molecular fuel injection. On the other hand, the SF_6 intercept is negative,
indicating a recombination loss of F atoms to below threshold requirements
in the channel prior to fuel injection.
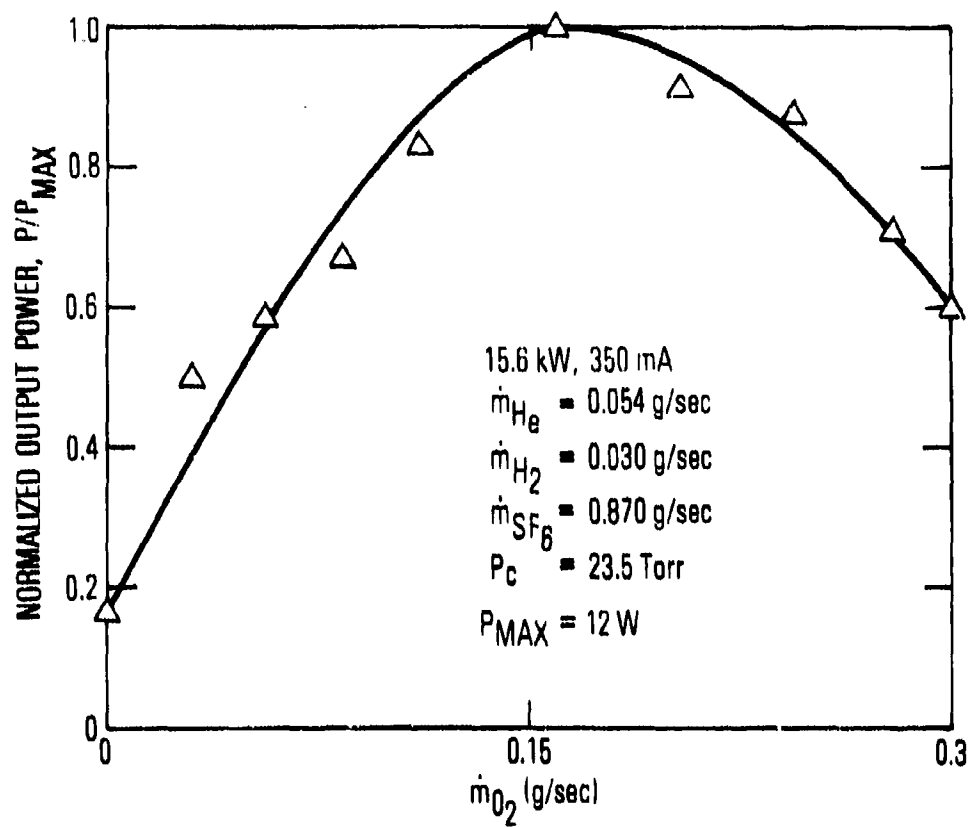
Figure 4. Variation of HF Laser Power with O_2 Mass Flow

Figure 5. Variation of HF Laser Power with He Mass Flow

The figure shows a plot of NORMALIZED OUTPUT POWER, P/P_{MAX} versus $\dot{m}_{He}$ (g/sec), with the following parameters:

15.6 kV, 350 mA

$\dot{m}_{H_2}$ = 0.030 g/sec

$\dot{m}_{O_2}$ ≈ 0.180 g/sec

$\dot{m}_{SF_6}$ = 0.870 g/sec

P_C = 23.5 Torr

P_{MAX} = 12 W
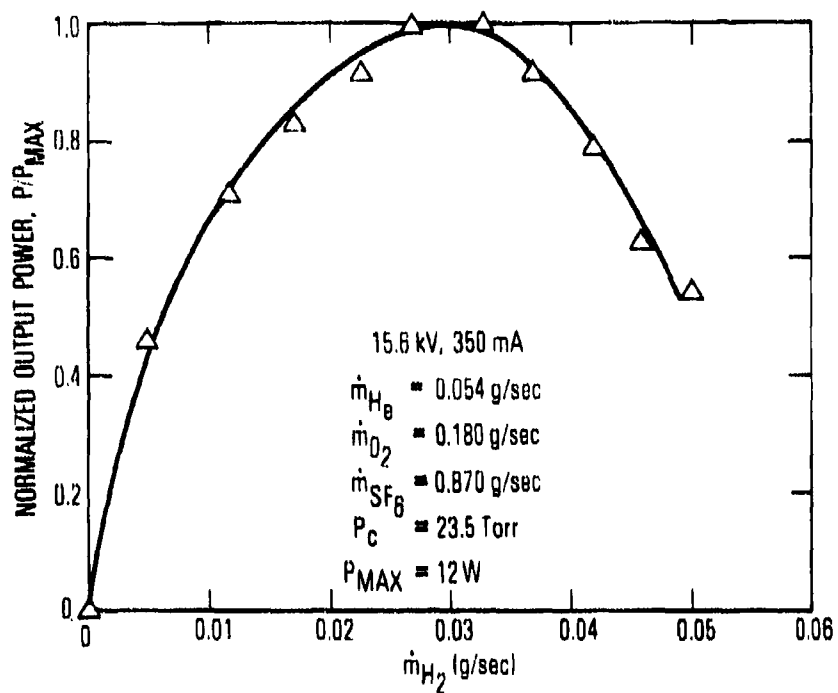
Figure 6. Variation of HF Laser Power with H$_2$ Mass Flow
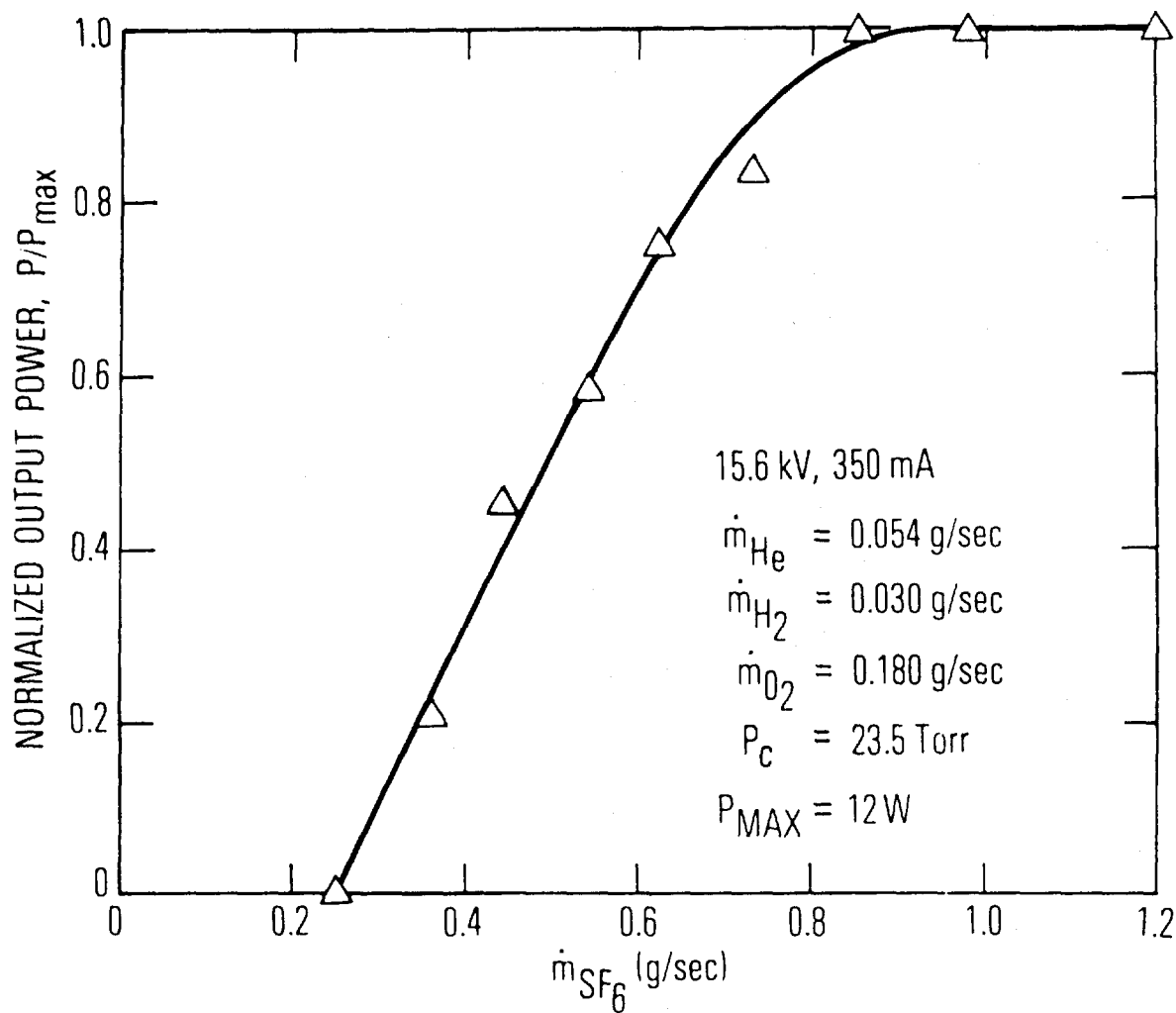
Figure 7. Variation of HF Laser Power with SF_6
Mass Flow

The figure is a plot of NORMALIZED OUTPUT POWER, P/P_{max} versus $\dot{m}_{SF_6}$ (g/sec), with the following annotations:

15.6 kV, 350 mA

$\dot{m}_{He} = 0.054$ g/sec

$\dot{m}_{H_2} = 0.030$ g/sec

$\dot{m}_{O_2} = 0.180$ g/sec

$P_c = 23.5$ Torr

$P_{MAX} = 12$ W

Figures 8, 9, 10, and 11 are normalized laser output curves for the various gases in DF laser operation. Only the SF_6 curve is identical to the HF counterpart. Comparison of the He curves for both HF and DF indicates a 16 versus 50% full-power zero-flow intercept. The O_2 curves for HF and DF indicate an even more dramatic difference in zero O_2 flow power (i.e., 16 versus 66%). Thus, the effect of He and O_2 is less pronounced for the DF laser than for the HF laser. Furthermore, the D_2 curve peaks at 0.7 times the molar flow of H_2. Detailed consideration of these differences in gas-flow power behavior between HF and DF lasers will be further studied.

Figure 8. Variation of DF Laser Power with O_2 Mass Flow

The figure shows normalized output power P/P_{MAX} versus $\dot{m}_{O_2}$ (g/sec) with the following parameters:

16.4 kV, 350 mA

$\dot{m}_{H_e}$ = 0.0405 g/sec

$\dot{m}_{D_2}$ = 0.044 g/sec

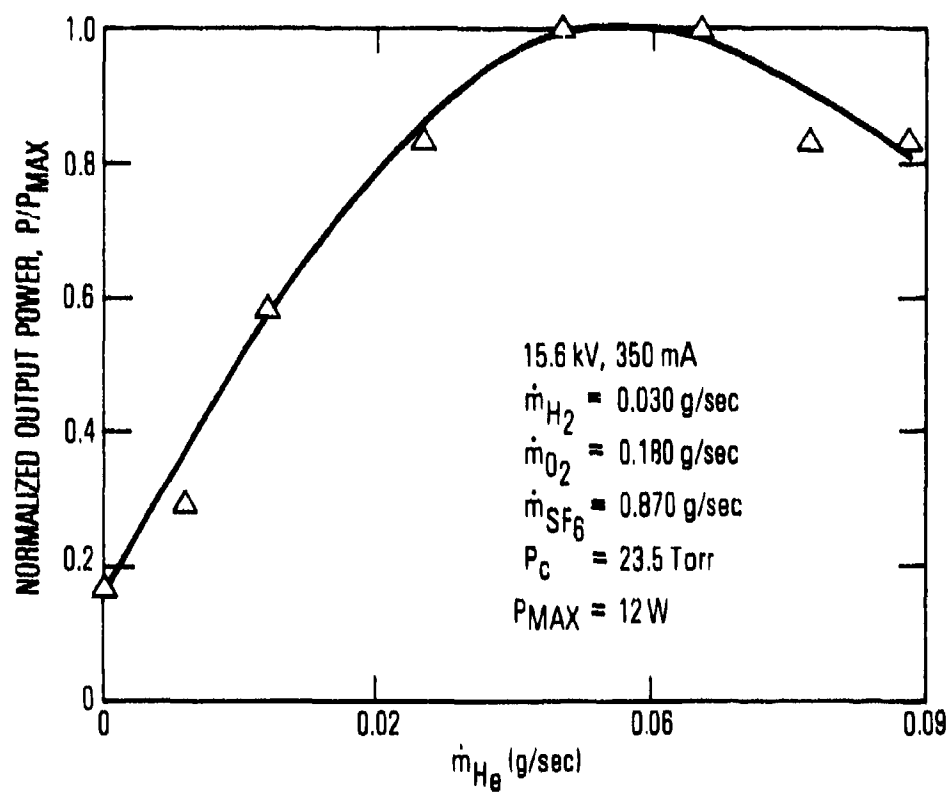$\dot{m}_{SF_6}$ = 0.980 g/sec

P_c = 24.0 Torr

P_{MAX} = 7 W

Figure 9. Variation of DF Laser Power with He
Mass Flow

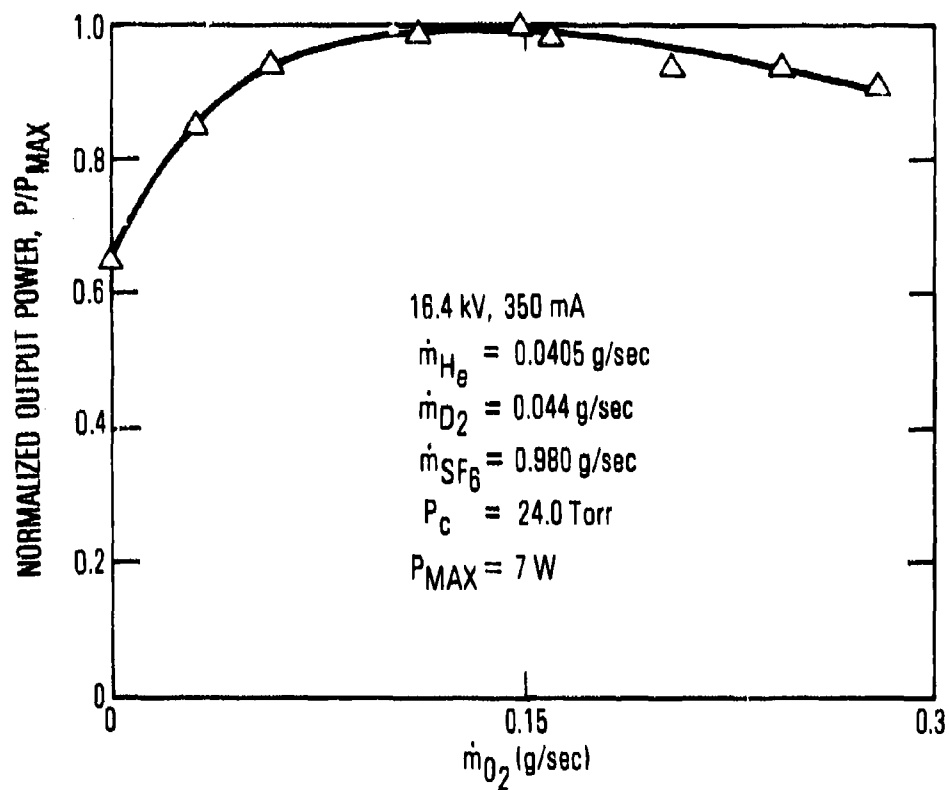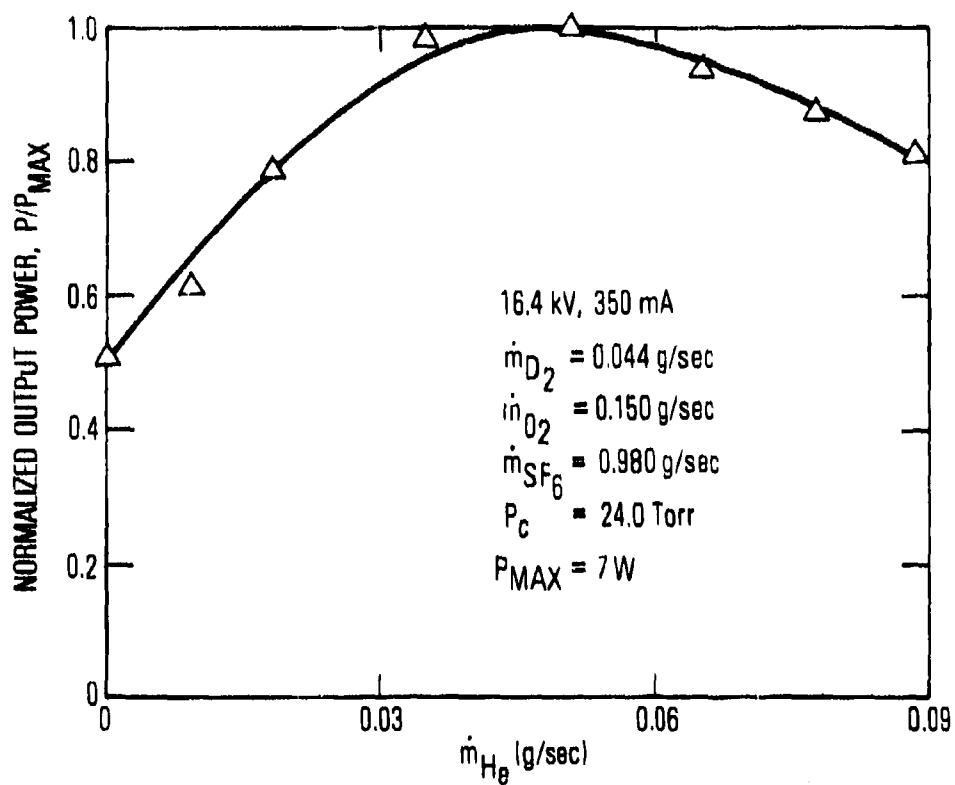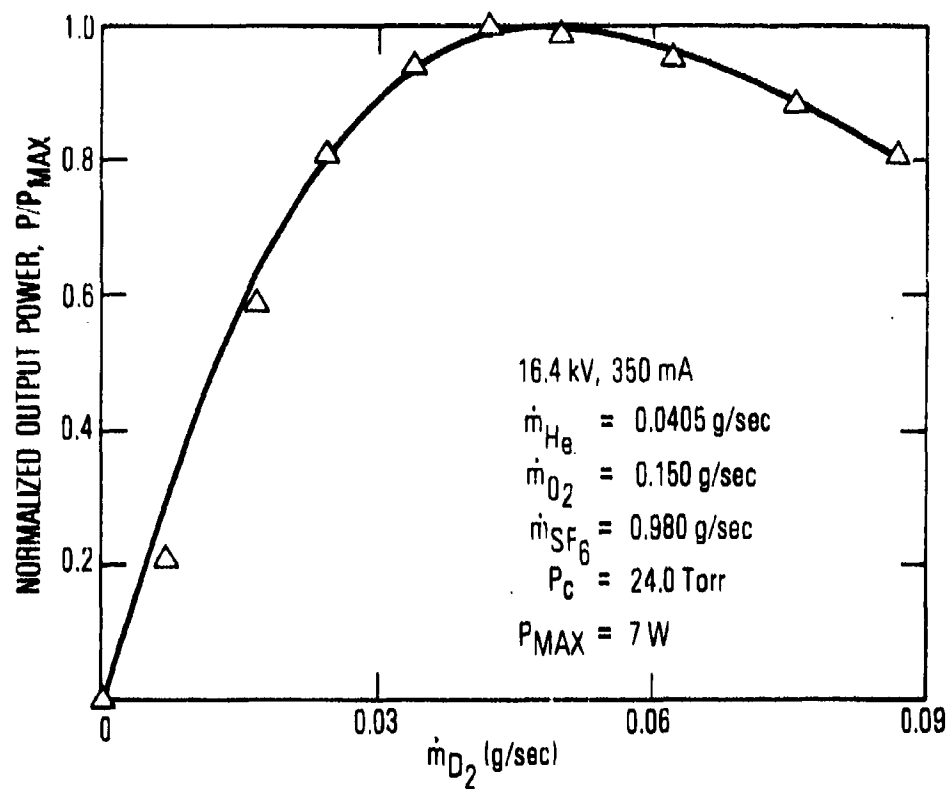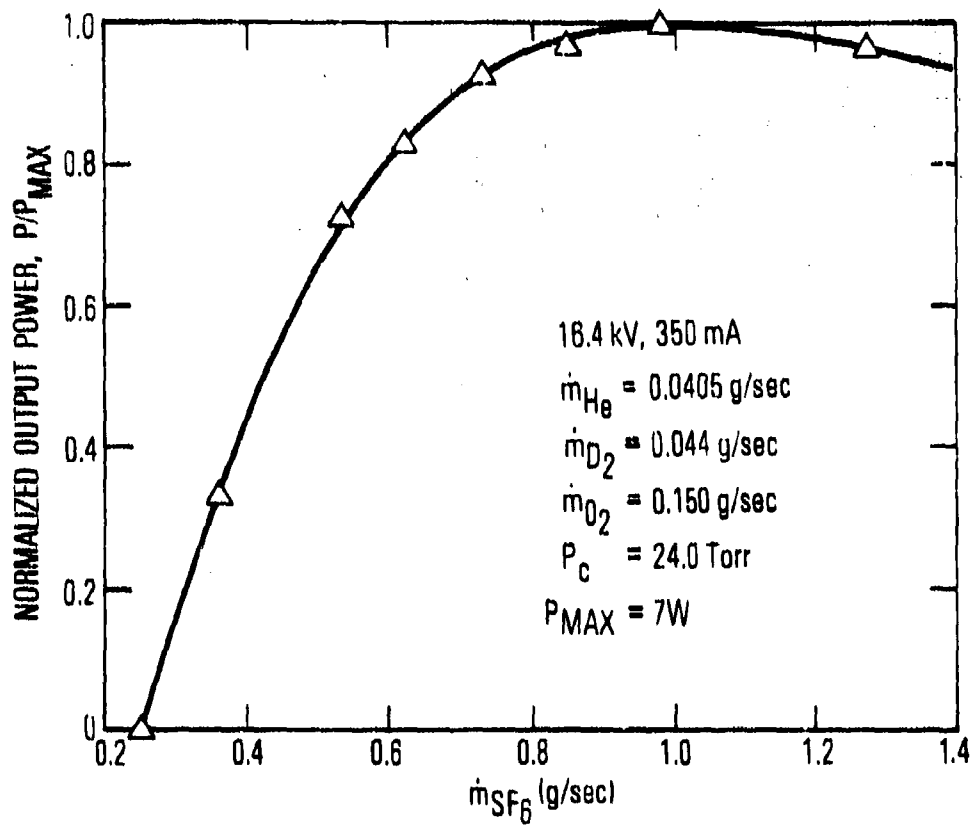Figure 10. Variation of DF Laser Power with D_2 Mass Flow

Figure 11.   Variation of DF Laser Power with SF_6 Mass Flow

IV. SINGLE-LINE PERFORMANCE

Diffraction-limited TEM_{oo} single-line laser beams are obtained directly from the laser cavity. Aperture-limiting of the lasing mode to TEM_{oo} is also employed but is generally not required. The laser beam is extracted as the grating zero-order beam. A PTR 92% efficient DF grating is used for power extraction for both HF and DF lines. The laser Brewster-angle windows are positioned to yield a vertically oriented E-vector that is parallel to the grating grooves for efficient HF operation. The laser lines and measured power obtained for each line at a distance 12 in. from the grating are given in Table IV. In addition, the power measurements obtained with the low-efficiency Bausch and Lomb replica grating ($\eta \sim 80\%$) are tabulated. Note that the $P_1(5)$ line is severely attenuated relative to other lines as a result of the strong atmospheric water vapor absorption. Eighteen lines are observed.

DF laser wavelengths and measured power levels obtained with the PTR 92% η grating are tabulated in Table V. DF lasing cannot be sustained on individual lines with the Bausch and Lomb replica grating.

Table IV. HF Laser Single-Line Performance

Line Designation P_v (j lower) v upper	Wavelength (μm)	Power PTR Grating (W)	Power Bausch and Lomb Grating (W)
$P_1(2)$	2.5788	0.12	0.02
(3)	2.6085	0.45	0.05
(4)	2.6398	1.50	0.12
(5)	2.6727	0.15	0.15
(6)	2.7075	1.50	0.30
(7)	2.7441	2.40	0.50
(8)	2.7826	1.40	0.40
(9)	2.8231	1.00	0.30
(10)	2.8657	0.30	0.10
$P_2(3)$	2.7275	0.20	0.05
(4)	2.7604	0.50	0.30
(5)	2.7853	1.30	0.62
(6)	2.8318	2.20	0.78
(7)	2.8706	2.20	0.95
(8)	2.9111	1.60	0.85
(9)	2.9539	0.90	0.70
(10)	2.9989	0.50	0.45
(11)	3.0461	0.30	0.20

Table V. DF Laser Single-Line Performance

Line Designation P (j lower) v upper	Wavelength (μm)	Power PTR Grating (W)
P_1(5)	3.5806	0.01
(6)	3.6128	0.025
(7)	3.6456	0.04
(8)	3.6798	0.10
(9)	3.7155	0.15
(10)	3.7520	0.20
(11)	3.7902	0.15
(12)	3.8298	0.10
(13)	3.8708	0.05
P_2(3)	3.6363	0.025
(4)	3.6665	0.06
(5)	3.6983	0.10
(6)	3.7310	0.15
(7)	3.7651	0.20
(8)	3.8007	0.25
(9)	3.8375	0.30
(10)	3.8757	0.32
(11)	3.9155	0.27
(12)	3.9565	0.20

Table V. DF Laser Single-Line Performance (Continued)

Line Designation P_v (j lower) v upper	Wavelength (μm)	Power PTR Grating (W)
$P_3(7)$	3.8903	0.01
(8)	3.9272	0.02
(9)	3.9654	0.05
(10)	4.0054	0.14
(11)	4.0464	0.07

V. LASER STABILITY

Amplitude stability is ~±1.5% for most HF lines. The DF lines
nearer threshold are more unstable, with most lines being amplitude-stable
to within ~±5%. The frequency stability of the laser is inferred initially from
frequency scans of individual lines containing a Lamb dip (Fig. 12).[6] The
clearly discernible Lamb dip feature in the trace indicates a frequency
stability an order of magnitude smaller than the average line width (i.e.,
approximately ±10 to 30 MHz). This natural-frequency stability estimate
has since been confirmed by a self-beating method[7] to be 30 MHz FWHM.
Line widths are typically ~400 MHz for HF and ~300 MHz for DF lines.
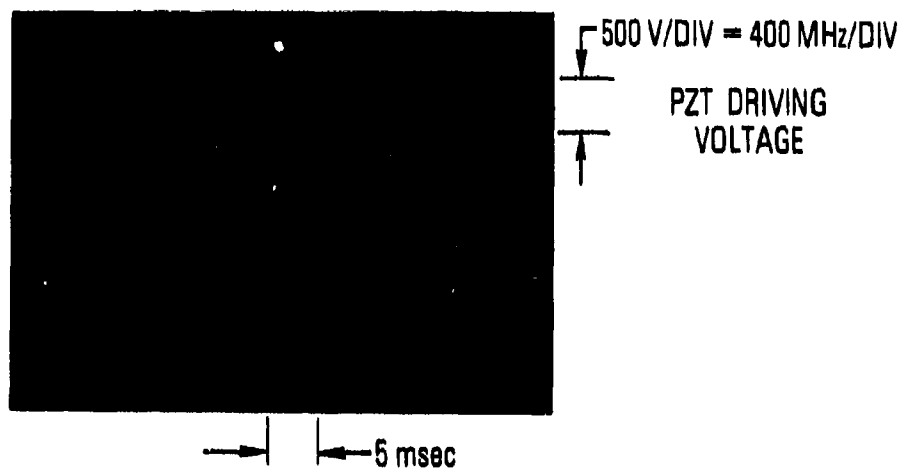
500 V/DIV = 400 MHz/DIV

PZT DRIVING
VOLTAGE

5 msec

Figure 12.   Frequency Scan of HF Laser Line $P_2(8)$
Showing Lamb Dip

VI. CONCLUDING REMARKS

This small-scale subsonic flow laser has been used extensively.
Applications of this laser to date include:

1. The diagnostic gain scanning of a 2.5-kW cw HF(DF) chemical laser.[2]

2. Sun-laser heterodyne radiometer transatmospheric transmission measurement, HF(DF).[3]

3. Absorption diagnostic probing for electron-beam pulse laser (HF).

4. The study of window-material absorption.

5. Maritime atmospheric-transmission measurement.

It is expected that the laser will be used in HF(DF) laser kinetic rate rate studies. Most of these investigations depend principally upon the single-line amplitude and frequency stability characteristics of the laser and generally require < 100 mW single-line power levels for adequate testing capability. Window material and optics coating studies, however, require higher power operation, and multiline performance is generally acceptable. In the event that power levels in excess of ~7 to 15 W are required, side-by-side operation of two (or more) laser body channels can be used in order to double (or more) the gain length of the flow contained in the laser cavity.

The nominal order of magnitude increase in output power in HF, the even greater increase in DF laser power, and the increased number of observable lines of this laser relative to Hinchen's[5] earlier laser appear to be derived principally from the use of increased mass flows and the power supply, and the vacuum pumping capability of the present laser.

REFERENCES

1. D. J. Spencer, H. Mirels, and D. A. Durran, "Performance of a CW HF Chemical Laser with N_2 or He Diluent," J. Appl. Phys. 43, 1151 (1972).

2. R. A. Chodzko, D. J. Spencer, H. Mirels, S. B. Mason, and D. H. Ross, "Zero-Power-Gain Measurements in CW HF(DF) Laser by Means of a Fast Scan Technique," IEEE J. Quantum Electron. QE-12, 660 (1976).

3. F. I. Shimabukuro, S. R. King, T. S. Hartwick, E. E. Reber, and D. J. Spencer, "Atmospheric Measurements at HF and DF Laser Wavelengths," Appl. Opt. 15, 1115 (1976).

4. T. A. Cool, R. R. Stephens, and J. A. Shirley, "HCl, HF and DF Partially Inverted CW Chemical Lasers", J. Appl. Phys. 41, 4038 (1970).

5. J. J. Hinchen, "Operation of a Small Single-Mode Stable CW Hydrogen Fluoride Laser," J. Appl. Phys. 45, 1818 (1974).

6. The oscilloscope trace is from R. L. Varwig, The Aerospace Corporation.

7. C. P. Wang, "Frequency Stability of a CW HF Chemical Laser," J. Appl. Phys. 47, 221 (1976).

THE IVAN A. GETTING LABORATORIES

The Laboratory Operations of The Aerospace Corporation is conducting experimental and theoretical investigations necessary for the evaluation and application of scientific advances to new military concepts and systems. Versatility and flexibility have been developed to a high degree by the laboratory personnel in dealing with the many problems encountered in the nation's rapidly developing space and missile systems. Expertise in the latest scientific developments is vital to the accomplishment of tasks related to these problems. The laboratories that contribute to this research are:

Aerophysics Laboratory: Launch and reentry aerodynamics, heat transfer, reentry physics, chemical kinetics, structural mechanics, flight dynamics, atmospheric pollution, and high-power gas lasers.

Chemistry and Physics Laboratory: Atmospheric reactions and atmospheric optics, chemical reactions in polluted atmospheres, chemical reactions of excited species in rocket plumes, chemical thermodynamics, plasma and laser-induced reactions, laser chemistry, propulsion chemistry, space vacuum and radiation effects on materials, lubrication and surface phenomena, photosensitive materials and sensors, high precision laser ranging, and the application of physics and chemistry to problems of law enforcement and biomedicine.

Electronics Research Laboratory: Electromagnetic theory, devices, and propagation phenomena, including plasma electromagnetics; quantum electronics, lasers, and electro-optics; communication sciences, applied electronics, semiconducting, superconducting, and crystal device physics, optical and acoustical imaging; atmospheric pollution; millimeter wave and far-infrared technology.

Materials Sciences Laboratory: Development of new materials; metal matrix composites and new forms of carbon; test and evaluation of graphite and ceramics in reentry; spacecraft materials and electronic components in nuclear weapons environment; application of fracture mechanics to stress corrosion and fatigue-induced fractures in structural metals.

Space Sciences Laboratory: Atmospheric and ionospheric physics, radiation from the atmosphere, density and composition of the atmosphere, aurorae and airglow; magnetospheric physics, cosmic rays, generation and propagation of plasma waves in the magnetosphere; solar physics, studies of solar magnetic fields; space astronomy, x-ray astronomy; the effects of nuclear explosions, magnetic storms, and solar activity on the earth's atmosphere, ionosphere, and magnetosphere; the effects of optical, electromagnetic, and particulate radiations in space on space systems.

THE AEROSPACE CORPORATION
El Segundo, California